Tomographic Methods for Universal Estimation in Quantum Optics

Scuola "E. Fermi", Varenna June 17-27, 2001

Giacomo Mauro D'Ariano

Istituto Nazionale di Fisica della Materia
Unità di Pavia, via Bassi 6, I-27100 Pavia, Italy

Index

1. Generalities

2. Homodyne tomography (continuous variables)

3. Pauli Tomography (qubits)

4. Examples and some experimental results.

5. Tomography of a Quantum Device.

6. Conclusions.

- ***Quantum Tomography*** is a method for estimating the ensemble average $\langle O \rangle$ of arbitrary operator of a quantum system from the measurement of a set—*quorum*—of (non commuting) observables.

- Measurements are performed, each observable at a time, on a ensemble of equally prepared quantum systems.

- We also want the possibility of unbiasing the estimation from instrumental noise.

- The quantum tomographic method can be extended to the estimation of the matrix form of any "quantum operation" (the quantum evolution in a device).

- General estimation problem: "Given a set of experimental measuring and transformation devices, which ensemble averages can be estimated?" Solution: mathematical theory based on *frames of operators* [look on quant-ph next months].

- Balanced homodyne detection

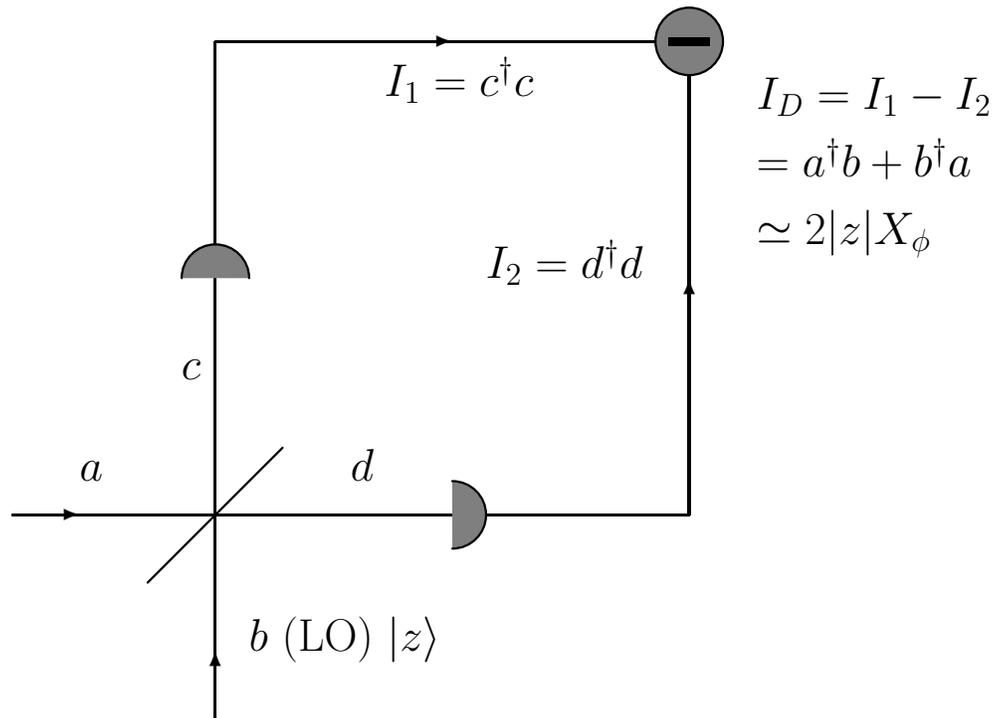Figure 1: Scheme of homodyne detection.

In the figure:

$$I_1 = c^\dagger c$$

$$I_2 = d^\dagger d$$

$$I_D = I_1 - I_2$$
$$= a^\dagger b + b^\dagger a$$
$$\simeq 2|z|X_\phi$$

c

a d

$b \ (\text{LO}) \ |z\rangle$

$$c = \frac{1}{\sqrt{2}}\left(a + b\right) \ , \quad d = \frac{1}{\sqrt{2}}\left(a - b\right) \ .$$

- In the *strong LO limit* $(z \to \infty)$ a balanced homodyne detector measures the quadrature X_ϕ of the field at any desired phase ϕ with respect to the local oscillator (LO)[1]

$$X_\phi = \frac{1}{2}\left(a^\dagger e^{i\phi} + a e^{-i\phi}\right)$$

[1]G. M. D'Ariano, *Quantum Estimation Theory and Optical Detection*, in *Concepts and Advances in Quantum Optics and Spectroscopy of Solids*, ed. by T. Hakioğlu and A. S. Shumovsky, (Kluwer Academic Publishers, Amsterdam 1997), p. 139-174 **lecture reprint available**

- Quantum efficiency:
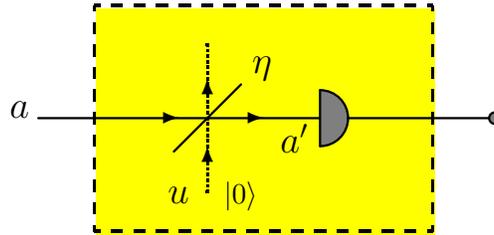

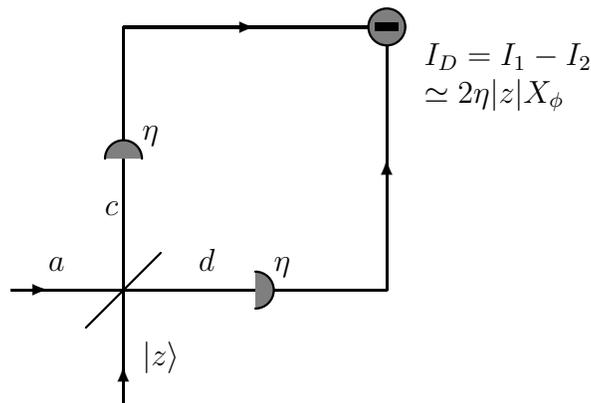Figure 2: Equivalence of a nonideal ($\eta < 1$) detector with an ideal one preceded by a beam splitter of transmissivity η.

$$I_D = I_1 - I_2 \simeq 2\eta|z|X_\phi$$

Figure 3: Homodyne detection with nonunit quantum efficiency η.

- Nonunit quantum efficiency $\eta < 1$ at detectors gives additional Gaussian noise with rms[2]

$$\Delta_\eta \equiv \sqrt{\frac{1-\eta}{4\eta}} \ .$$

[2]G. M. D'Ariano, *Quantum Estimation Theory and Optical Detection*, in *Concepts and Advances in Quantum Optics and Spectroscopy of Solids*, ed. by T. Hakioğlu and A. S. Shumovsky, (Kluwer Academic Publishers, Amsterdam 1997), p. 139-174

lecture reprint available

Homodyne Tomography

- The first technique to reconstruct the density matrix from homodyne measurements, originated from the following idea[1] the collection of probability distributions $\{p(x;\phi)\}_{\phi\in[0,\pi)}$ of the quadratures for varying ϕ is just the Radon transform of the Wigner function $W(\alpha,\overline{\alpha})$.

$$p(x;\phi) = \int_{-\infty}^{+\infty} dy\, W\left((x+iy)e^{i\phi},(x-iy)e^{-i\phi}\right) \; ;$$

- Wigner function:

$$W(\alpha,\overline{\alpha}) = \int \frac{d^2\lambda}{\pi^2} e^{\alpha\bar{\lambda}-\bar{\alpha}\lambda} \mathrm{Tr}\left(\hat{\rho}e^{\lambda a^\dagger - \bar{\lambda}a}\right) \; .$$

- Then, by inverting the Radon transform, one obtains the Wigner function

$$W(\alpha,\overline{\alpha}) = \int_{-\infty}^{+\infty} \frac{dr|r|}{4} \int_0^\pi \frac{d\phi}{\pi} \int_{-\infty}^{+\infty} dx\, p(x;\phi)\exp\left[ir(x-\alpha_\phi)\right]$$

where $\boxed{\alpha_\phi = \mathrm{Re}(\alpha e^{-i\phi}).}$

- From the knowledge of $W(\alpha,\overline{\alpha})$ one can recover the matrix elements of the density operator $\hat{\varrho}$

$$\langle x+x'|\hat{\rho}|x-x'\rangle = \int_{-\infty}^{\infty} dy\, e^{2ix'y} W(x+iy, x-iy) \; ,$$

$$\rho_{nm} = \sqrt{\frac{2^{1-n-m}}{\pi n!m!}} \int_{-\infty}^{\infty} dx \int_{-\infty}^{\infty} dx'\, e^{-(x^2+x'^2)} H_n(\sqrt{2}x) H_m(\sqrt{2}x')\, \langle x|\hat{\rho}|x'\rangle \; ,$$

[1] K. Vogel and H. Risken, Phys. Rev. A **40**, 2847 (1989). D. T. Smithey, M. Beck, M. G. Raymer, and A. Faridani, Phys. Rev. Lett. **70**, 1244 (1993).
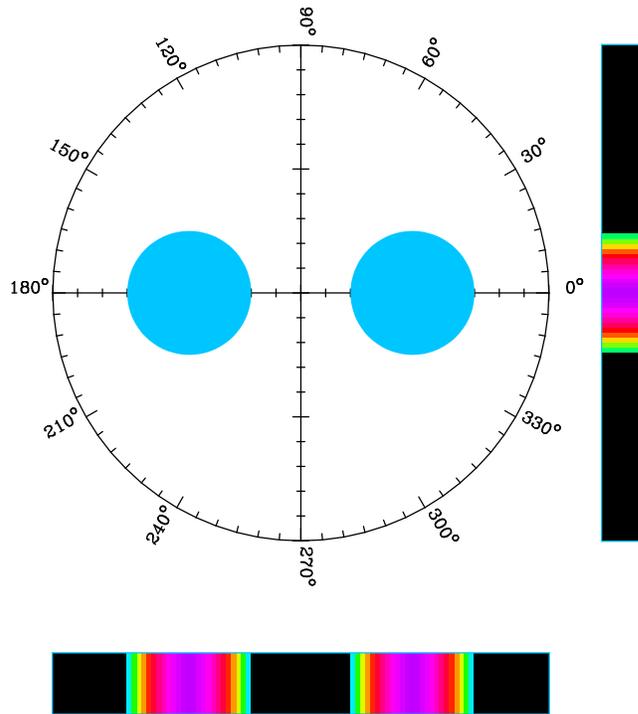
- *Imaging and tomography*

Figure 4: Illustration of a tomography machine

- A **tomography** of a two dimensional image $W(\alpha, \bar{\alpha})$ is a collection of one dimensional projections $p(x; \phi)$ at different values of the observation angle ϕ.

$$W(\alpha, \overline{\alpha}) = \int_{-\infty}^{+\infty} \frac{dr\,|r|}{4} \int_{0}^{\pi} \frac{d\phi}{\pi} \int_{-\infty}^{+\infty} dx\, p(x; \phi) \exp\left[ir(x - \alpha_\phi)\right] \ .$$
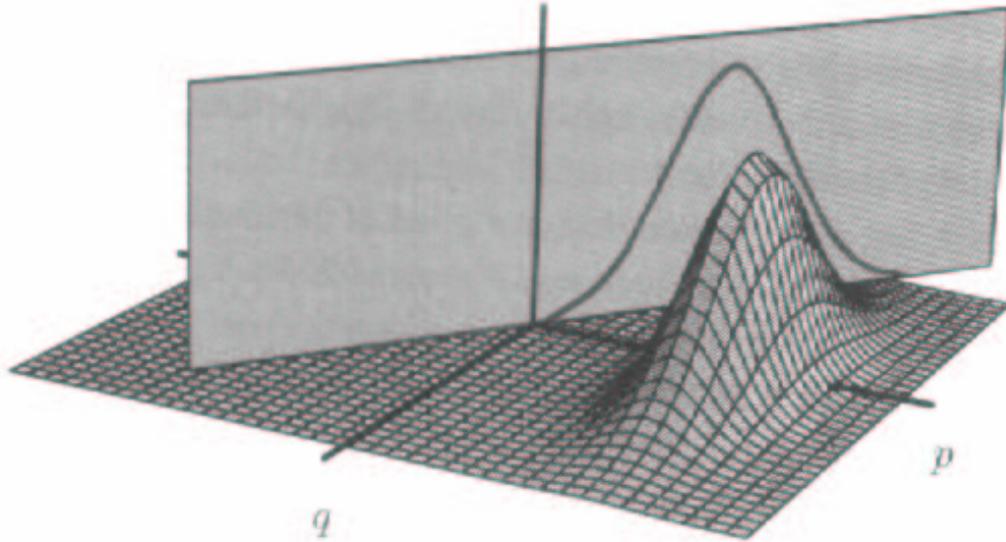
Figure 5: From: U. Leonhardt, *Measuring the Quantum State of Light*, Cambridge University Press (1997)

3

$$
\begin{aligned}
W(\alpha, \overline{\alpha}) &= \int_{-\infty}^{+\infty} \frac{dr|r|}{4} \int_0^{\pi} \frac{d\phi}{\pi} \int_{-\infty}^{+\infty} dx \, p(x; \phi) \exp\left[ir(x - \alpha_\phi)\right] = \\
&= (-\partial_{\alpha\overline{\alpha}}^2)^{\frac{1}{2}} \int_0^{\phi} \mathrm{d}\phi \, p(\mathrm{Re}(\alpha e^{-i\phi}), \phi) \, .
\end{aligned}
$$

[3]G. M. D'Ariano, *Measuring Quantum States*, in *Quantum Optics and Spectroscopy of Solids*, ed. by T. Hakioğlu and A. S. Shumovsky, (Kluwer Academic Publisher, Amsterdam 1997), p. 175-202[4]

lecture reprint available

Homodyne Tomography

- ## Limitations of the tomographic method:

It is impossible to obtain the Wigner function by averaging:

$$W(\alpha, \overline{\alpha}) = \int_0^\pi \frac{d\phi}{\pi} \int_{-\infty}^{+\infty} dx \, p(x; \phi) \left[-\frac{1}{2} P \frac{1}{(x - \alpha_\phi)^2} \right] \ ,$$

$$P \frac{1}{z^2} \equiv \lim_{\varepsilon \to 0^+} \mathrm{Re} \frac{1}{(z + i\varepsilon)^2} \ , \qquad \alpha_\phi = \mathrm{Re}(\alpha e^{-i\phi}) \ .$$

$W(\alpha, \overline{\alpha})$ is the average over data (distributed according to $p(x; \phi)$, with random phase ϕ) of an **unbounded kernel**.

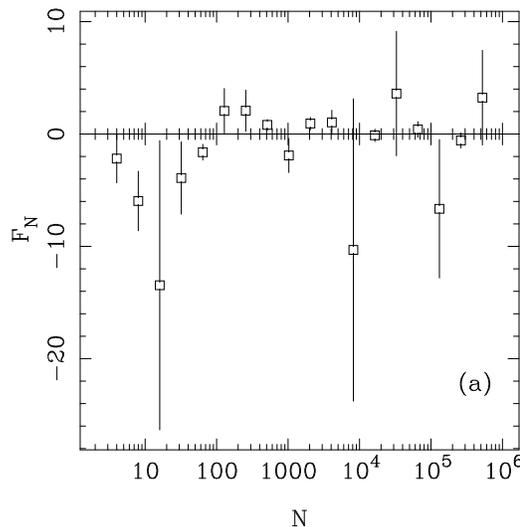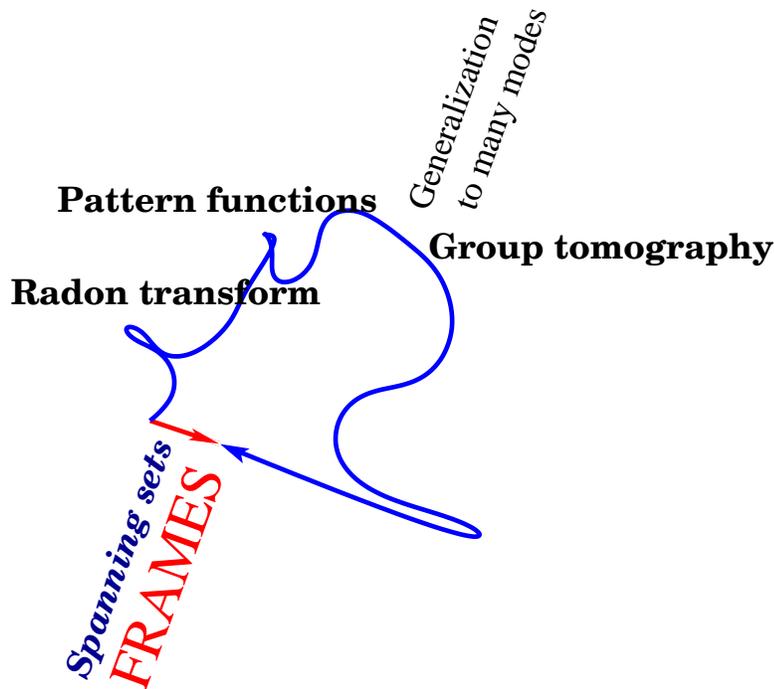- The conditions for the central limit theorem are not fulfilled.

Figure 6: Numerical simulation of experiments for estimating the "average" of $f(x) = \frac{1}{x}$ with uniform probability $p(x) = 1/2$ for $x \in [-1, 1]$.

History of quantum tomography

Radon Transform $\Longrightarrow$ Pattern Functions[2] $\Longrightarrow$ Deconvolving quantum efficiency[3] $\Longrightarrow$ Many modes[4] $\Longrightarrow$ Universal estimation [5] $\Longrightarrow$ Group Tomography and general noise deconvolution [6] [7] $\Longrightarrow$ Max-likelihood [8] $\Longrightarrow$ Spanning sets[9] [10] $\Longrightarrow$ **Theory of Frames of Observables**[11]

[2] **G. M. D'Ariano, C. Macchiavello and M. G. A. Paris**, Phys. Rev. A **50** 4298 (1994).

[3] G. M. D'Ariano, U. Leonhardt and H. Paul, Phys. Rev. A **52** R1801 (1995).

[4] G. M. D'Ariano, P. Kumar, M. Sacchi, Phys. Rev. A **61**, 13806 (2000).

[5] G. M. D'Ariano, in *Quantum Communication, Computing, and Measurement*, Edited by O. Hirota, A. S. Holevo, and C. M. Caves, Plenum Publishing (New York and London 1997), p. 253.

[6] G. M. D'Ariano, in *Quantum Communication, Computing, and Measurement 2*, Edited by P. Kumar, G. M. D'Ariano, and O. Hirota, Kluwer Academic/Plenum Publishers (New York and London 2000), p. 137.

[7] G. M. D'Ariano, Phys. Lett. A **268** 151 (2000).

[8] K. Banaszek, G. M. D'Ariano, M. G. A. Paris, M. Sacchi, Phys. Rev A **61**, 010304 (2000).

[9] G. M. D'Ariano, L. Maccone, and M. Paris, Phys. Rev. A (2001)

[10] G. Cassinelli, G. M. D'Ariano, E. De Vito, A. Levrero, J. Math. Phys. **41** 7940 (2000)

[11] **G. M. D'Ariano, quant-ph to appear next months**

- **Exact method:** bypass the evaluation of $W(\alpha, \overline{\alpha})$!

  - The displacement operators $D(\alpha) = e^{\alpha a^{\dagger} - \alpha^* a}$ for $\alpha \in \mathbb{C}$ are a orthonormal basis for the operator Hilbert Schmidt space, since $\text{Tr}[D^{\dagger}(\beta)D(\alpha)] = \pi \delta^{(2)}(\alpha - \beta)$. One has the expansion

$$H = \int \frac{\mathrm{d}^2 \alpha}{\pi} \text{Tr}[HD(\alpha)]D^{\dagger}(\alpha) \ .$$

  - Change to polar variables: $\alpha = \frac{i}{2} k e^{i\phi}$:

$$H = \int_0^{2\pi} \frac{\mathrm{d}\phi}{\pi} \int_0^{+\infty} \frac{\mathrm{d}k \, k}{4} \text{Tr}[He^{ikX_\phi}]e^{-ikX_\phi} \ .$$

  - Take the ensemble average of both sides, and write the ensemble average $\langle H \rangle$ as the double average of an **estimator** $E_H(X_\phi; \phi)$ over ϕ and over the ensemble:

$$\langle H \rangle = \int_0^{2\pi} \frac{\mathrm{d}\phi}{2\pi} \langle E_H(X_\phi; \phi) \rangle \ ,$$

  where

$$E_H(x; \phi) \doteq \frac{1}{2} \int_0^{+\infty} \mathrm{d}k \, k \, \text{Tr}[He^{ikX_\phi}]e^{-ikx} \ .$$

  - Use the symmetry $X_{-\phi} = -X_\phi$, and get:

$$\begin{aligned}
\langle H \rangle &= \int_0^{\pi} \frac{\mathrm{d}\phi}{\pi} \langle E_H(X_\phi; \phi) \rangle \ , \\
E_H(x; \phi) &= \frac{1}{4} \int_0^{\infty} \mathrm{d}t \, \text{Tr}\left[H \cos \sqrt{t}(X_\phi - x)\right] \\
&\equiv \frac{1}{4} \int_{-\infty}^{+\infty} \mathrm{d}k \, |k| \text{Tr}[He^{ikX_\phi}]e^{-ikx} \ ,
\end{aligned}$$

Homodyne Tomography

- ## Unbiasing noise

  - Gaussian noise from nonunit quantum efficiency Γ_η give:

  $$\Gamma_\eta(\exp(ikX_\phi)) = \exp(ikX_\phi)e^{-\frac{1-\eta}{8\eta}k^2} \ ,$$

  - The tomographic estimation can be "unbiased", by finding an estimator $E_H^{(\eta)}(x; \phi)$ such that

  $$\langle H \rangle = \int_0^\pi \frac{\mathrm{d}\phi}{\pi} \langle E_H^{(\eta)}(X_\phi; \phi) \rangle_\eta \ ,$$

  where $\langle \ldots \rangle_\eta$ denotes the *experimental* ensemble average, i. e. with the noisy state ${}^t\Gamma_\eta(\rho)$.

  - One has:

  $$E_H^{(\eta)}(X_\phi; \phi) \doteq \Gamma_\eta^{-1}\{E_H(X_\phi)\} = \frac{1}{4}\int_{-\infty}^{+\infty}\mathrm{d}k\,|k|e^{\frac{1-\eta}{8\eta}k^2}\mathrm{Tr}[He^{ikX_\phi}]e^{-ikX_\phi} \ .$$

- Example: matrix element $\rho_{n+d,n}$: $\boxed{H = |n\rangle\langle n + d|}$

- Derivation:

$$
\begin{aligned}
E_{|n\rangle\langle n+d|}^{(\eta)}(x; \phi) &= \frac{1}{4}\int_0^\infty \mathrm{d}t\, e^{\frac{1-\eta}{8\eta}t}\mathrm{Tr}\left[|n\rangle\langle n + d|\cos\sqrt{t}(X_\phi - x)\right] = \\
&= \frac{1}{8}\int_0^\infty \mathrm{d}t\, e^{-\frac{2\eta-1}{8\eta}t - i\sqrt{t}x}\langle n + d|{:}e^{i\sqrt{t}X_\phi}{:}|n\rangle + \mathrm{c.c} = \\
&= \frac{i^d}{8}e^{id\phi}\sqrt{\frac{n!}{(n+d)!}}\int_0^\infty \mathrm{d}t\, e^{-\frac{2\eta-1}{8\eta}t - i\sqrt{t}x}\, t^{l/2}L_n^d(t) + \mathrm{c.c}
\end{aligned}
$$

- bounded for $\eta > \eta_b = \frac{1}{2}$.

- A more efficient algorithm uses factorization formulas [Richter, Leonhardt] and Bernoulli convolution inversion.

- ## Estimators:

- The estimator $E^{(\eta)}_{|n\rangle\langle n+d|}(x;\phi)$ of the matrix element $\rho_{n+d,n}$ has a bounded range which does not depend on n and depends very weakly on d.

- It oscillates increasingly fast for increasing n and d.

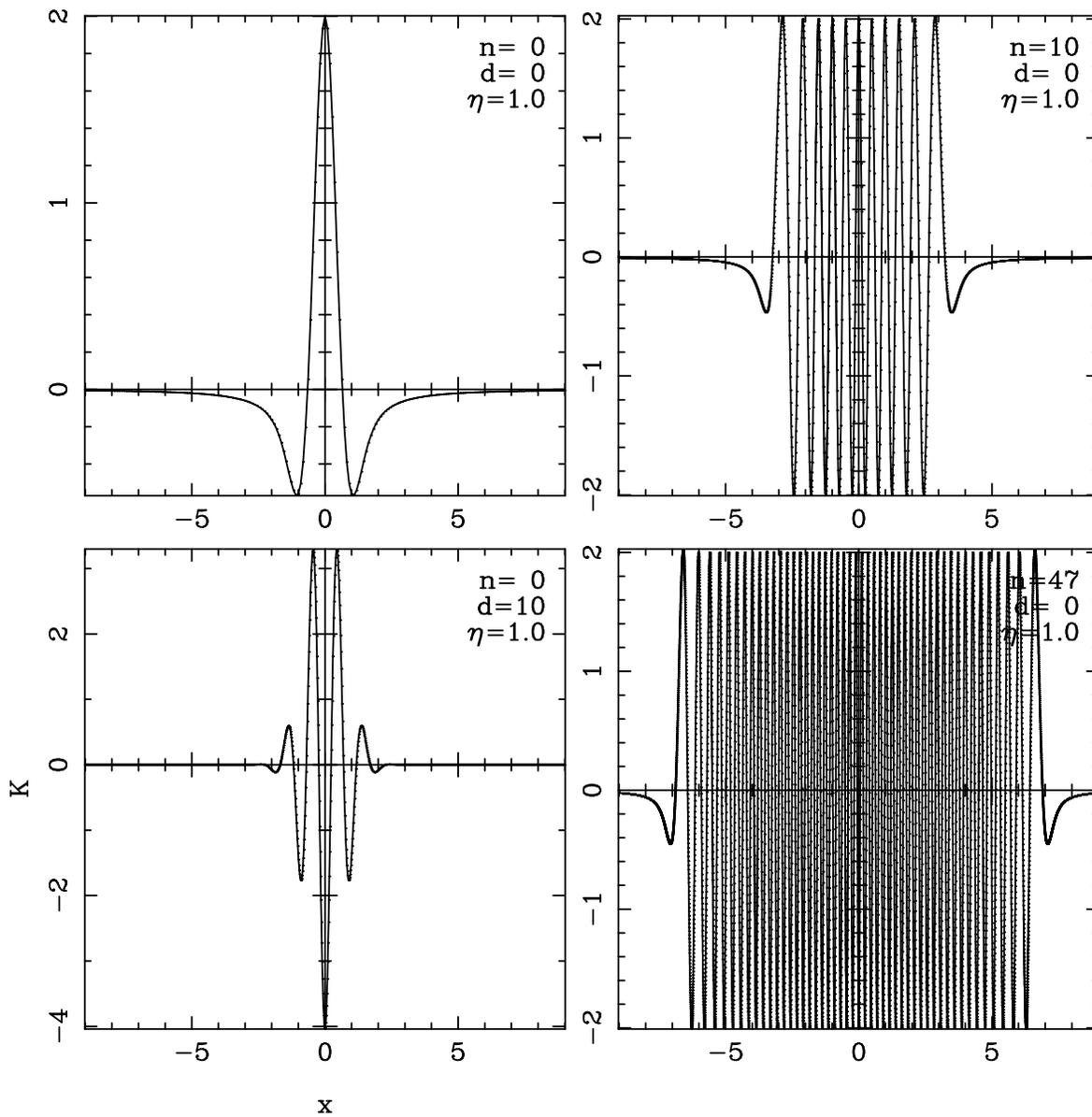- Hence, errors will increase versus n, d, but will remain bounded.

Figure 7: Estimator $E^{(\eta)}_{|n\rangle\langle n+d|}(x;\phi)$ of the matrix element $\rho_{n+d,n}$ for $\eta = 1$

- **Estimators:**

- The estimator of $\rho_{n+d,n}$ has a bounded range whose amplitude increases fast versus n, d, and η.

- Hence, errors will increase versus n, d, and η.
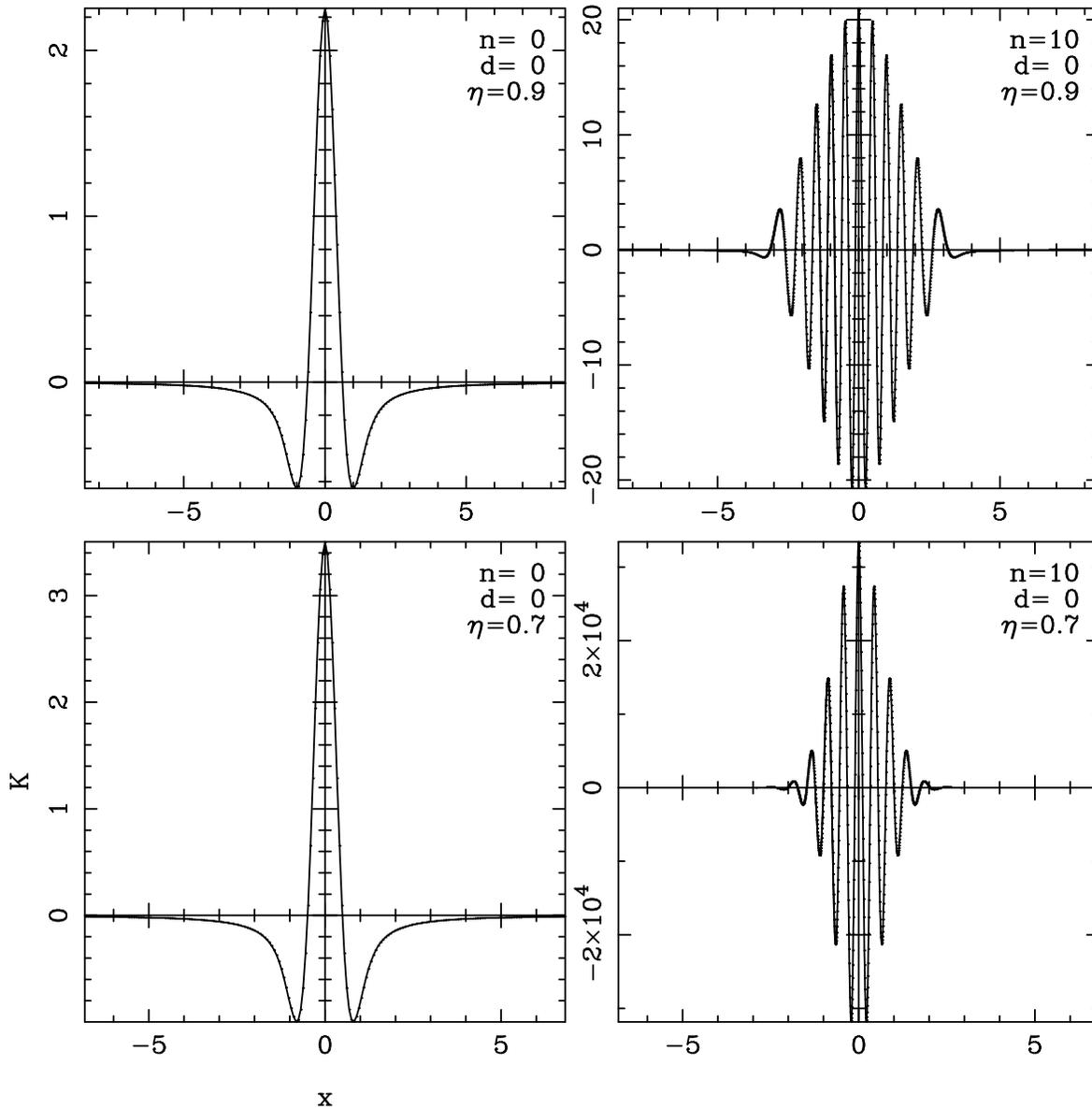

Figure 8: Estimator $E^{(\eta)}_{|n\rangle\langle n+d|}(x;\phi)$ of the matrix element $\rho_{n+d,n}$ for $\eta < 1$

Homodyne tomography

- ## Estimators: Statistical errors

  For $n \gg (2\eta - 1)/(1 - \eta)$ and $\eta < 1$ one approximately has the variance:

  $$\sigma^2[\rho_{n,n}] \simeq \frac{\eta^{3/2}}{\sqrt{\pi(1-\eta)}n} \, e^{\frac{1}{4n}\frac{(2\eta-1)^2}{\eta(1-\eta)}} \left(\frac{1}{2\eta-1}\right)^{2n+1} .$$

- For $\eta = 1$, one has $\sigma^2[\rho_{n,n}] \simeq \sqrt{2}$.

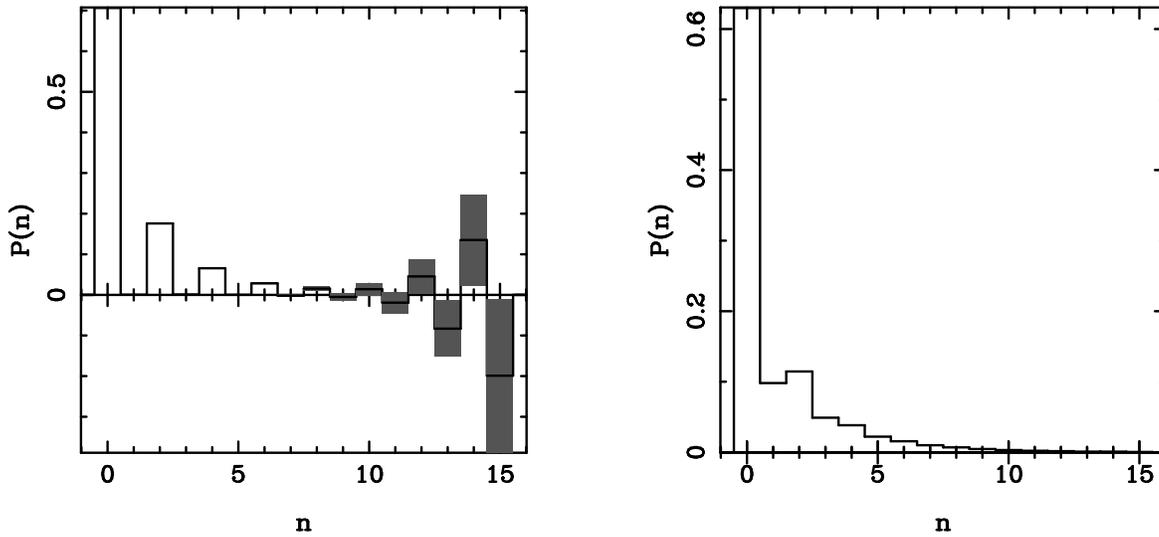- **Monte Carlo simulations:** Schleich–Wheeler oscillations.

Figure 9: Tomographic reconstruction of the photon-number probability of a squeezed vacuum ($\langle a^\dagger a \rangle = 1$) with detection efficiency $\eta = .8$. Homodyne data are computer simulated. [Here we averaged over 27 phases using 200 blocks of 5×10^5 data for each phase]. Experimental errors (confidence intervals) are represented by the gray-shaded thickness of horizontal lines. Left: unbiased reconstruction. Right: reconstruction without unbiasing.
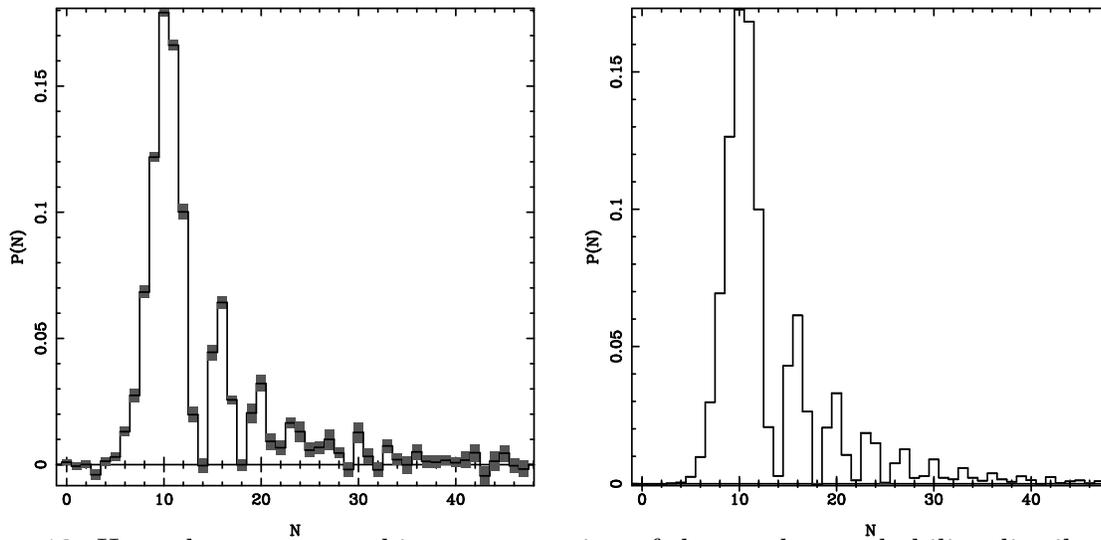

Figure 10: Homodyne tomographic reconstruction of the number probability distribution for a squeezed state. Simulation with 10 data blocks of 260 phases with 100 measurement each (left) 100 data block of 2600 phases with 100 measurement each (right)

Homodyne Tomography

- **Notice:** Measuring the density matrix elements $\rho_{n,m}$ is not equivalent to measure the ensemble average of any desired observable. In fact, for infinite-dimensional Hilbert spaces **we need convergence of experimental errors**

$$\langle H \rangle = \sum_{n,m} \varrho_{n,m} H_{n,m} \,, \text{ with errors } \varepsilon^2[H] \simeq \sum_{n,m} \varepsilon^2[\rho_{n,m}] \, |H_{n,m}|^2 \,.$$

If $|H_{n,m}|^2$ doesn't vanish properly, the estimation of $\langle H \rangle$ is affected by a **diverging error**

- Analogously, we have **experimental inequivalence of representations**: statistical measurement errors make different representations of the state experimentally inequivalent.

Consider two different complete orthonormal sets $\{|n\rangle\}$ and $\{|\lambda\rangle\}$. If we measure $\varrho_{n,m} \doteq \langle n|\varrho|m\rangle$, we generally cannot obtain the matrix element $\varrho_{\mu,\nu} \doteq \langle \mu|\varrho|\nu\rangle$ from $\varrho_{n,m}$ as follows

$$\varrho_{\mu,\nu} = \sum_{nm} \langle m|\nu\rangle\langle\mu|n\rangle \varrho_{n,m} \,,$$

if the **series of errors** don't converge

$$\varepsilon^2[\varrho_{\mu,\nu}] = \sum_{nm} |\langle m|\nu\rangle\langle\mu|n\rangle|^2 \varepsilon^2[\varrho_{n,m}] \,,$$

- Conclusion: **bypass the measurement of $\varrho_{n,m}$!**

- **What about non-traceclass operators?**

  - The expansion in displacement operators cannot be used:

  $$H = \int \frac{\mathrm{d}^2\alpha}{\pi} \mathrm{Tr}[HD(\alpha)]D^\dagger(\alpha) \ .$$

- A systematic method for finding estimators for a large class of operators is to change the definition of scalar product [**theory of frames**]. Also, by analytic methods [Richter] one can find easily expansions of the form:

  $$
  \begin{aligned}
  E_a^{(\eta)}(X_\phi;\phi) &= 2e^{i\phi}X_\phi \ , \\
  E_{a^\dagger a}^{(\eta)}(X_\phi;\phi) &= 2X_\phi^2 - \frac{1}{2\eta} \ ,
  \end{aligned}
  $$

  - and, more generally:

  $$\mathcal{E}_{:a^{\dagger m}a^n:_s}^{(\eta)}(X_\phi;\phi) = e^{i(n-m)\phi}\frac{H_{m+n}\left(\sqrt{\frac{2}{s_\eta}}X_\phi\right)}{\binom{n+m}{n}\left(\sqrt{2/s_\eta}\right)^{n+m}} \ , \quad s_\eta \doteq s - 1 + \eta^{-1}$$

  - Example of "renormalized" expansion:

  $$H = \int_0^\pi \frac{\mathrm{d}\phi}{\pi} \int_{-\infty}^\infty \mathrm{d}t \, \mathrm{Tr}[HG_{t,\phi}^\dagger]F_{t,\phi}$$

  where

  $$
  \begin{aligned}
  F_{t,\phi} &= \frac{1}{\sqrt{2\pi}} \exp\left[2(X_\phi + it/2)^2\right] \\
  G_{t,\phi}^\dagger &= \frac{\mathrm{d}}{\mathrm{d}t}t \int_0^1 \mathrm{d}\theta \, \exp[\theta(1-\theta)t^2]\, e^{-ie^{i\phi}\theta t a^\dagger}\, |0\rangle\langle 0|\, e^{-ie^{-i\phi}(1-\theta)ta}
  \end{aligned}
  $$

Homodyne Tomography

- **Generalization to two modes:** estimators for tensor products factorize

$$E^{(\eta)}_{H_1 \otimes H_2}(x_1, x_2; \phi_1, \phi_2) = E^{(\eta)}_{H_1}(x_1; \phi_1) \times E^{(\eta)}_{H_2}(x_2; \phi_2) ,$$

  - By linearity extend to any operator on $\mathsf{H} \otimes \mathsf{H}$, and find the full joint density matrix or any ensemble average for any <u>entangled</u> state, by just using local joint homodyne measurements.

- Correlations come from joint homodyne probability $p(x_1, x_2; \phi_1, \phi_2)$!

Homodyne Tomography

- **Improvements:**

- **"Adaptive" schemes**, based on non unicity of estimators (existence of "null estimators"). Estimators are "adapted to data" via least squares method.

- In general, choose coefficients μ and ν in order to minimize the error:

$$K_H^{(\eta)}(x;\phi) = E_H^{(\eta)}(x;\phi) + \mu \cdot \mathcal{F}(x;\phi) + \nu \cdot \mathcal{F}^*(x;\phi) ,$$

where

$$\mathcal{F}(x;\phi) \doteq \{x^k \exp[i(2n+2+k)\phi]\}$$

- $\overline{\Delta(K_H^{(\eta)})^2}$ minimum $\Rightarrow$

$$\mathbf{A}\mu = \mathbf{b} , \qquad \mathbf{A}\nu = \mathbf{c} ,$$
$$\mathbf{A} = \overline{\mathcal{F}\mathcal{F}^*} , \qquad \mathbf{b} = -\overline{\mathcal{E}_\eta[A]\mathcal{F}^*} , \qquad \mathbf{c} = -\overline{\mathcal{E}_\eta[A]\mathcal{F}} .$$

- The statistical error is reduced by the amount

$$\overline{\Delta(K^{(\eta)})^2} - \overline{\Delta(E^{(\eta)})^2} = -\mathbf{b} \cdot \mathbf{A}^{-1}\mathbf{b}^* - \mathbf{c} \cdot \mathbf{A}^{-1}\mathbf{c}^* .$$

- Example: $H = a^\dagger a$, for coherent, squeezed vacuum, and Schrődinger-cat states.

$$E_{a^\dagger a}^{(\eta)}(x;\phi) = 2x^2 - \frac{1}{2} + 2\mathrm{Re}[\mu \exp(2i\phi)] ,$$
$$\mu = -\overline{2x^2 \exp(2i\phi)} \equiv -\frac{1}{2}\langle a^{\dagger 2}\rangle ,$$

$$\overline{\Delta(E_{a^\dagger a}^{(\eta)})^2} \equiv \langle\Delta(a^\dagger a)^2\rangle + \frac{1}{2}[\langle a^{\dagger 2}a^2\rangle - \underbrace{\langle a^{\dagger 2}\rangle\langle a^2\rangle}_{\text{noise reduction}} + 2\langle a^\dagger a\rangle + 1] .$$

- **Improvements:**

- **Max-likelihood strategy** (for density matrix only).

 - Write the density matrix by in the Cholevsky form: $\rho = \tau^\dagger \tau$.

 - Find the maximum of the likelihood:

$$L(\tau) = \sum_{i=1}^{N} \log \mathrm{Tr}\left[\tau^\dagger \tau \, \Gamma_\eta \left(|x_i\rangle_{\phi_i \phi_i}\langle x_i|\right)\right] - N \, \mathrm{Tr}(\tau^\dagger \tau) \,,$$

$$\mathrm{Tr}\left[\tau^\dagger \tau \, \Gamma_\eta \left(|x_i\rangle_{\phi_i \phi_i}\langle x_i|\right)\right]$$
$$= \sum_{k=0}^{M-1} \sum_{j=0}^{k} \left| \sum_{n=0}^{k-j} \sqrt{\binom{n+j}{n}} \eta^n (1-\eta)^j \langle k|\tau|n+j\rangle \langle n|x_i\rangle e^{in\phi_i} \right|^2 \,.$$

- Method biased: need truncation of Hilbert space.

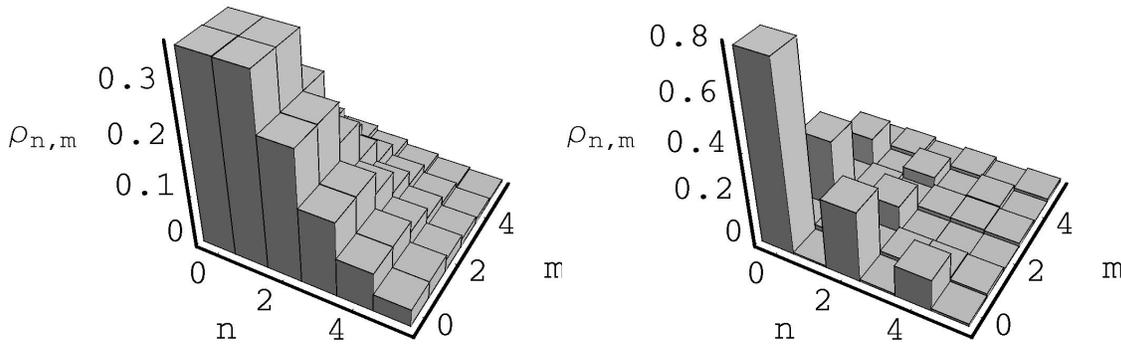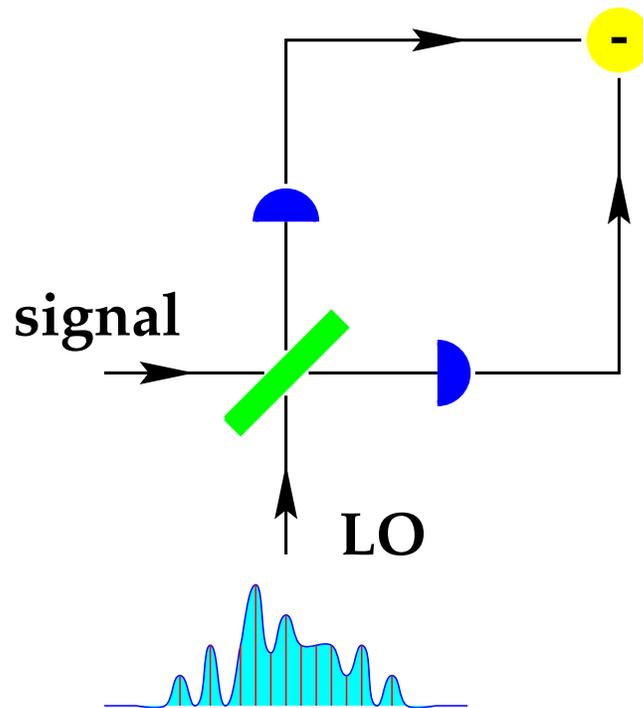- Complexity growing exponentially with the number of modes.

Figure 11: Fig. 1: Monte Carlo simulation of the tomographic reconstruction of the density matrix using the maximum likelihood technique. Left: density matrix for a coherent state with $\langle a^\dagger a \rangle = 1$; Right: squeezed vacuum with $\langle a^\dagger a \rangle = 0.5$. Both: 100 phases with 5000 data each. Hilbert space truncation set to $N_H = 5$; quantum efficiency $\eta = 0.8$

- **one-LO multimode homodyne tomography:**

- **Multimode field**, with annihilation operators $a_1, a_2, \ldots, a_{n+1}$

- Quadratures:

$$X(\theta, \psi) = \frac{1}{2} \left[A^\dagger(\theta, \psi) + A(\theta, \psi) \right] \ , \psi_l \in [0, 2\pi] \ , \theta_l \in [0, \pi] \ ,$$

$$A(\theta, \psi) = \sum_{l=0}^{n} e^{-i\psi_l} u_l(\theta) a_l \ , \vec{u}(\theta) \in S^n \ .$$

- averaging over ψ and θ with probability measure:

$$\mathrm{d}\mu(\theta, \psi) = n! \prod_{l=0}^{n} \frac{\mathrm{d}\psi_l}{2\pi} \, \mathrm{d}\theta_l \, \sin^{2(n-l)+1} \frac{\theta_l}{2} \, \cos \frac{\theta_l}{2} \ .$$

- **one-LO multimode homodyne tomography:**

  - Estimator:

$$E_H^{(\eta)}(X(\theta, \psi); \theta, \psi) = \frac{\kappa^{n+1}}{n!} \int_0^\infty \mathrm{d}t\, t^n\, e^{i2\sqrt{\kappa t}X(\theta,\psi)} \mathrm{Tr}[A e^{-i2\sqrt{\kappa t}X(\theta,\psi)}] \ .$$

  $\kappa = \frac{2\eta}{2\eta-1}$.

- Matrix element $\langle\{n_l\}|R|\{m_l\}\rangle$ of the **joint density matrix of modes:**

$$E_{|\{m_l\}\rangle\langle\{n_l\}|}^{(\eta)}(x; \theta, \psi) =$$

$$e^{-i\sum_{l=0}^n (n_l-m_l)\psi_l} \frac{\kappa^{n+1}}{n!} \prod_{l=0}^n \left\{ [-i\sqrt{\kappa}u_l(\theta)]^{\mu_l-\nu_l} \sqrt{\frac{\nu_l!}{\mu_l!}} \right\}$$

$$\times \int_0^\infty \mathrm{d}t\, e^{-t+2i\sqrt{\kappa t}x}\, t^{n+\frac{1}{2}\sum_{l=0}^n (\mu_l-\nu_l)} \prod_{l=0}^n L_{\nu_l}^{\mu_l-\nu_l}[\kappa u_l^2(\theta)t] \ ,$$

  - $\mu_l = \max(m_l, n_l)$, $\nu_l = \min(m_l, n_l)$.

- Probability distribution of the total number of photons $\boxed{N = \sum_{l=0}^n a_l^\dagger a_l}$

$$\boxed{E_{|p\rangle\langle p|}^{(\eta)}(x; \theta, \psi) = \frac{\kappa^{n+1}}{n!} \int_0^\infty \mathrm{d}t\, e^{-t+2i\sqrt{\kappa t}x}\, t^n L_p^n[\kappa t] \ ,}$$

  - $|p\rangle$ eigenvector of N for eigenvalue p.
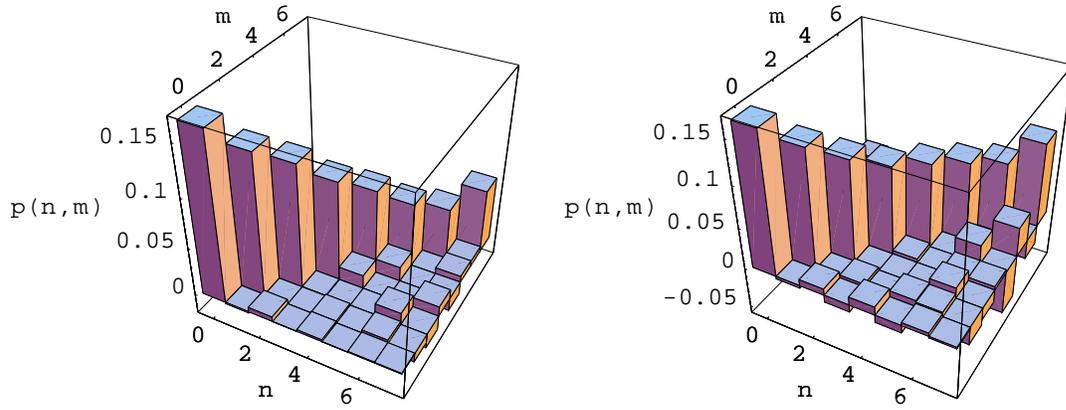
Figure 12: Two-mode photon-number probability $p(n,m)$ of the twin-beam state of parametric fluorescence for average number of photons per beam $\overline{n} = |\xi|^2/(1 - |\xi|^2) = 5$ obtained by a Monte-Carlo simulation with random parameters $\cos 2\theta$, ψ_1, and ψ_2. On the left we have quantum efficiency $\eta = 1$, and a sample of 10^6 data has been used. On the right quantum efficiency is $\eta = .9$, and a sample of $5 * 10^6$ data has been used.
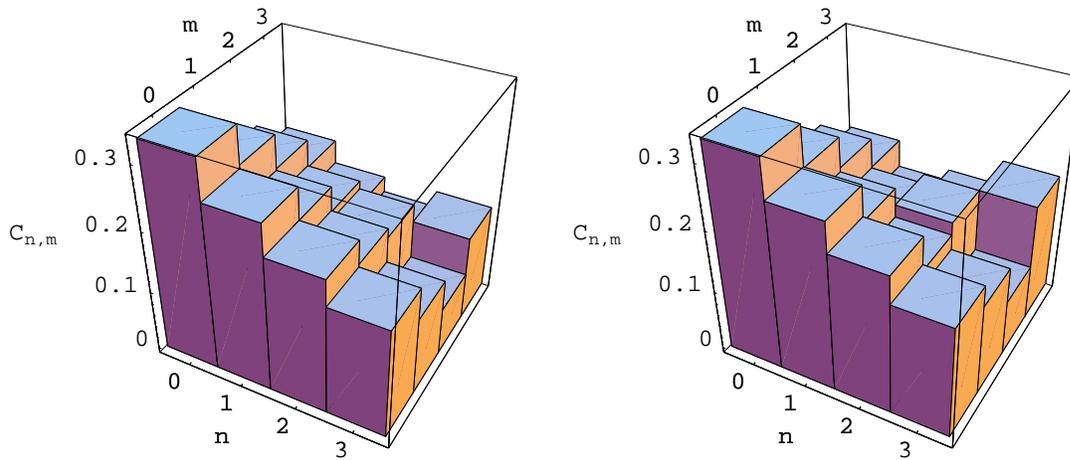

Figure 13: Tomographic reconstruction of the matrix elements $C_{n,m} \equiv {}_a\langle m|_b\langle m|\Psi\rangle\langle\Psi|n\rangle_a|n\rangle_b$ of the twin-beam state of parametric fluorescence for average number of photons per beam $\overline{n} = 2$. On the left we have quantum efficiency $\eta = .9$, and a sample of 10^6 data has been used. On the right quantum efficiency is $\eta = .8$, and a sample of $3 * 10^6$ data has been used.

- M. Vasilyev, S.-K. Choi, P. Kumar, and G. M. D'Ariano, *Tomographic Measurement of Joint Photon Statistics of the Twin-Beam Quantum State*, Phys. Rev. Lett. **84** 2354 (2000)

- First measurement of the joint photon-number probability distribution for a two-mode quantum state created by a nondegenerate optical parametric amplifier.

- The measured distributions exhibit up to 1.9 dB of quantum correlation between the signal and idler photon numbers, whereas the marginal distributions are thermal as expected for parametric fluorescence.
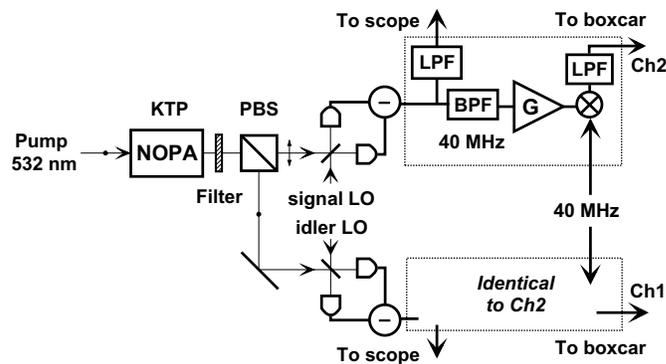

Figure 14: A schematic of the experimental setup. NOPA, non-degenerate optical parametric amplifier; LOs, local oscillators; PBS, polarizing beam splitter; LPFs, low-pass filters; BPF, band-pass filter; G, electronic amplifier. Electronics in the two channels are identical.
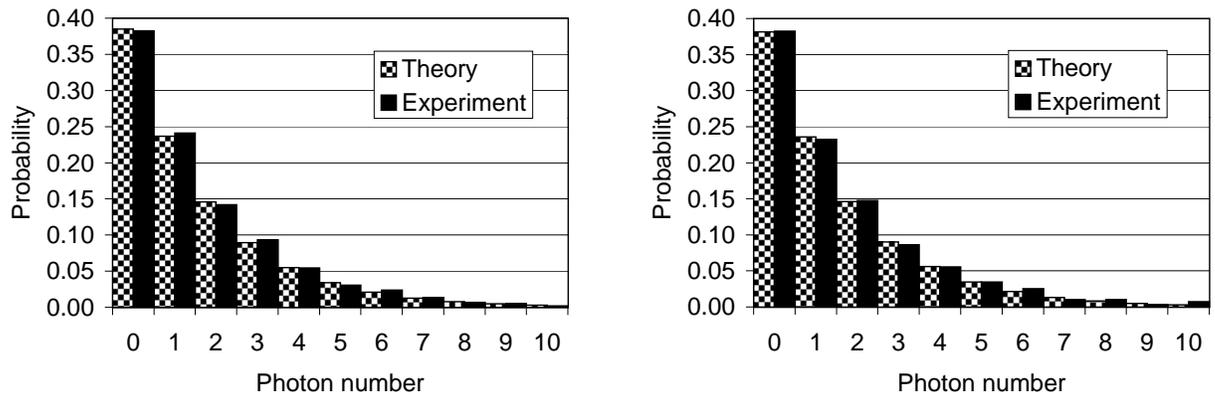
Figure 15: Marginal distributions for the signal and idler beams. Theoretical distributions for the same mean photon numbers are also shown.
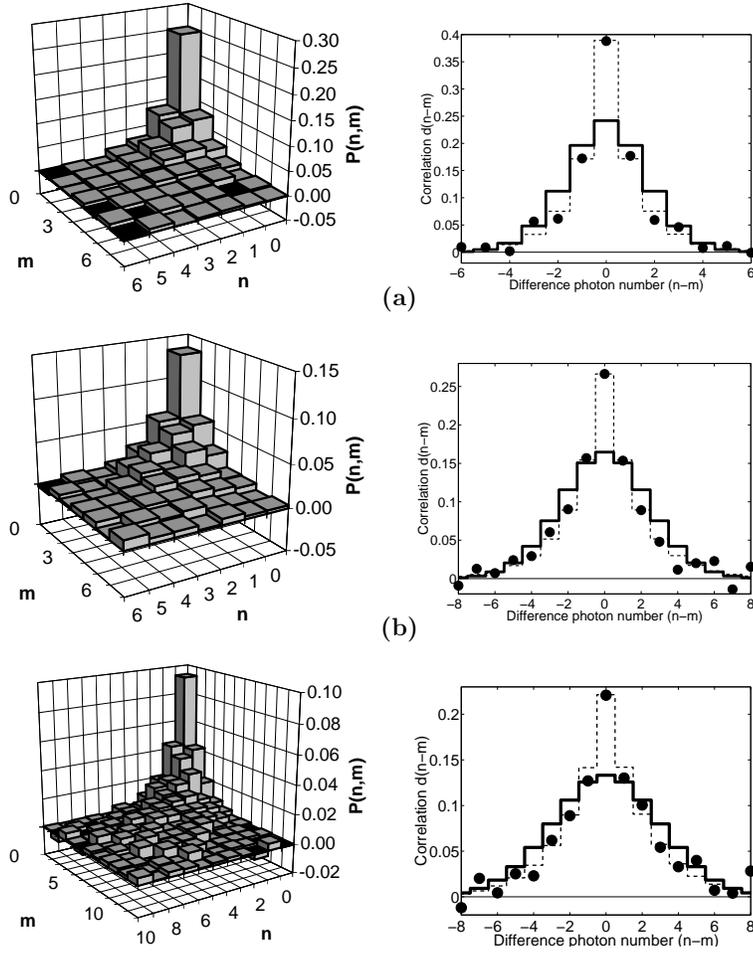
Figure 16: Left: Measured joint photon-number probability distributions for the twin-beam state. Right: Difference photon number distributions corresponding to the left graphs. Filled circles: experimental data; solid lines: theoretical predictions; dashed lines, difference photon-number distributions for two independent coherent states with the same total mean number of photons and $\bar{n} = \bar{m}$. (a) 400000 samples, $\bar{n} = \bar{m} = 1.5$, $N = 10$; (b) 240000 samples, $\bar{n} = 3.2$, $\bar{m} = 3.0$, $N = 18$; (c) 640000 samples, $\bar{n} = 4.7$, $\bar{m} = 4.6$, $N = 16$.

Pauli matrices with identity I , σ_x , σ_y , σ_z: orthonormal basis for the qubit operator space:

$$H = \frac{1}{2}\{\vec{\sigma} \cdot \text{Tr}[\vec{\sigma}H] + I\,\text{Tr}[H]\} \ .$$

• Tomographic estimation:

$$\langle H \rangle = \frac{1}{3} \sum_{\alpha=x,y,z} \langle E_H(\sigma_\alpha;\alpha)\rangle \ ,$$

$$E_H(\sigma_\alpha;\alpha) = \frac{3}{2}\text{Tr}[H\sigma_\alpha]\sigma_\alpha + \frac{1}{2}\text{Tr}[H]$$

- Unbiasing noise. Example: "Pauli channel" $(0 \le p \le 1)$:

$$\Gamma_p(H) = (1-p)H + \frac{p}{2}\text{Tr}[H] \ ,$$

$$E_H^{(p)}(\sigma_\alpha;\alpha) = \frac{3}{2(1-p)}\text{Tr}[H\sigma_\alpha]\sigma_\alpha + \frac{1}{2}\text{Tr}[H]$$

- Qubit realized by polarization of single photon states.

$$\sigma_z = h^\dagger h - v^\dagger v,$$
$$|\uparrow\rangle \equiv |1\rangle_h |0\rangle_v, \ |\downarrow\rangle \equiv |0\rangle_h |1\rangle_v,$$

$$\sigma_y = e^{i\frac{\pi}{4}\sigma_x} \sigma_z e^{-i\frac{\pi}{4}\sigma_x} \ ,$$

$$e^{-i\frac{\pi}{4}\sigma_x} |1\rangle_h |0\rangle_v = \frac{1}{\sqrt{2}} [|1\rangle_h |0\rangle_v - i|0\rangle_h |1\rangle_v] \equiv |1\rangle_l |0\rangle_r \ ,$$

$$\sigma_x = e^{-i\frac{\pi}{4}\sigma_y} \sigma_z e^{i\frac{\pi}{4}\sigma_y} \ ,$$

$$e^{i\frac{\pi}{4}\sigma_y} |1\rangle_h |0\rangle_v = \frac{1}{\sqrt{2}} [|1\rangle_h |0\rangle_v - |0\rangle_h |1\rangle_v] \equiv |1\rangle_\nearrow |0\rangle_\searrow \ .$$
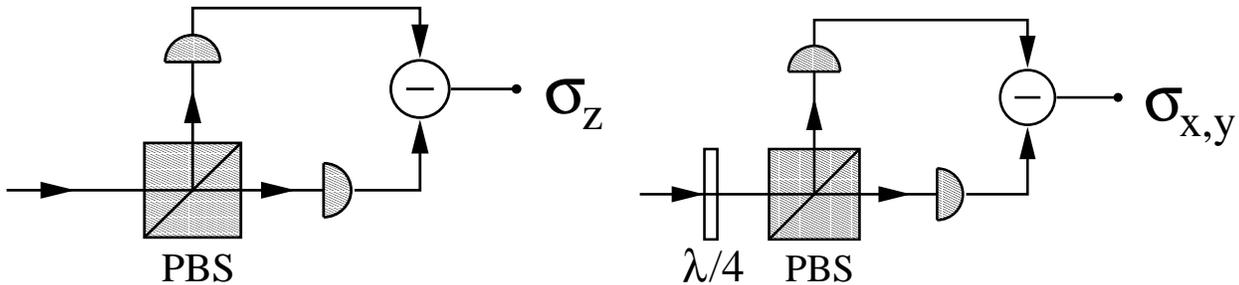

Figure 17: Pauli-matrix detectors for photon-polarization qubits.

- Quantum operations are the most general state evolutions in quantum mechanics.

- The *input* and *output* states are connected via the map

$$\rho \rightarrow \frac{\mathrm{E}(\rho)}{\mathrm{Tr}(\mathrm{E}(\rho))} \, ,$$

which occurs with probability $\mathrm{Tr}(\mathrm{E}(\rho)) \leq 1$

- The *quantum operation* E is a linear, trace-decreasing CP-map.

- Suppose that we have a quantum machine that performs an unknown quantum operation E, and we want to determine E experimentally. How can we do?

- We can exploit the one-to-one correspondence E $\leftrightarrow R_{\mathrm{E}}$ between quantum operations on $\mathsf{S}(\mathsf{H})$ and positive operators R_{E} on $\mathsf{H} \otimes \mathsf{H}$.

$$R_{\mathrm{E}} = \mathrm{E} \otimes \mathsf{I}_{\mathsf{H}}(|I\rangle\!\rangle\langle\!\langle I|) \, ,$$
$$\mathrm{E}(\rho) = \mathrm{Tr}_2[I \otimes {}^{\mathrm{t}}\rho R_{\mathrm{E}}] \, ,$$

- $O \sum_{nm} O_{nm}|n\rangle\langle m|$

  ${}^{\mathrm{t}}O = \sum_{nm} O_{mn}|n\rangle\langle m|$ transposed operator

  $O^* = \sum_{nm} O_{nm}^*|n\rangle\langle m|$ conjugate operator

- $|v\rangle = \sum_n v_n|n\rangle$

  $|v^*\rangle = \sum_n v_n^*|n\rangle$ conjugate vector

- $\mathsf{HS}(\mathsf{H})$ Hilbert space of Hilbert-Schmidt operators on H

  $\langle A, B\rangle \doteq \mathrm{Tr}[A^\dagger B],$

  $||A||_{HS}^2 \doteq \mathrm{Tr}[A^\dagger A].$

- Isomorphism $\mathsf{HS}(\mathsf{H}) \simeq \mathsf{H} \otimes \mathsf{H}$:

  $$|A\rangle\!\rangle \doteq \sum_{nm} A_{nm}|n\rangle \otimes |m\rangle \equiv A \otimes I|I\rangle\!\rangle \equiv I \otimes {}^{\mathrm{t}}A|I\rangle\!\rangle \,,$$

  $$\langle\!\langle A|B\rangle\!\rangle \equiv \mathrm{Tr}[A^\dagger B] \doteq \langle A, B\rangle \,,$$

  $$A \otimes B|C\rangle\!\rangle = |AC\,{}^{\mathrm{t}}B\rangle\!\rangle \,.$$
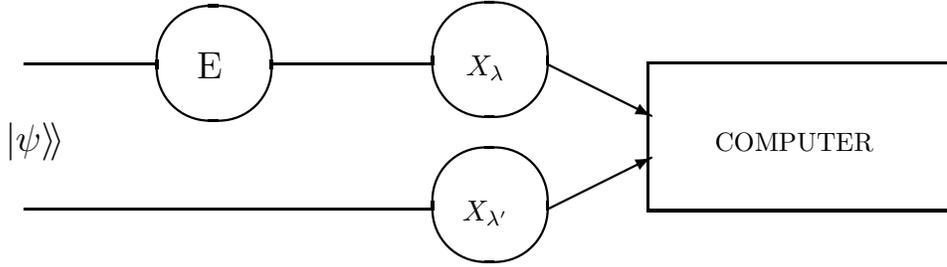
Figure 18: General experimental scheme of the method for the tomographic estimation of a quantum operation. Two identical quantum systems are prepared in an entangled state $|\psi\rangle\!\rangle$. One of the two systems undergoes the quantum operation E, whereas the other is left untouched. At the output one makes a quantum tomographic estimation, photocurrent by measuring jointly two random observables from a quorum $\{X_\lambda\}$.

- If we consider an entangled input state $|\psi\rangle\!\rangle$ and operate only one one side with the quantum operation, the output state is the joint density matrix

$$|\psi\rangle\!\rangle\langle\!\langle\psi| \;\rightarrow\; R(\psi) \equiv \mathrm{E} \otimes \mathrm{I}(|\psi\rangle\!\rangle\langle\!\langle\psi|) \;.$$

- The quantum operation E is in correspondence with $R_\mathrm{E} \equiv R(\psi)$ for $\psi = I$, and for invertible ψ the two matrices $R(I)$ and $R(\psi)$ are connected as follows

$$R(I) = (I \otimes \psi^{-1T})R(\psi)(I \otimes \psi^{-1*}) \;.$$

Hence, the quantum operation (four-index) matrix R_E can be obtained by estimating via quantum tomography the following output ensemble averages

$$\langle\!\langle i,j|R(I)|l,k\rangle\!\rangle = \langle\; |l\rangle\langle i| \otimes |\psi^{-1*}(k)\rangle\langle\psi^{-1*}(j)| \;\rangle \;.$$
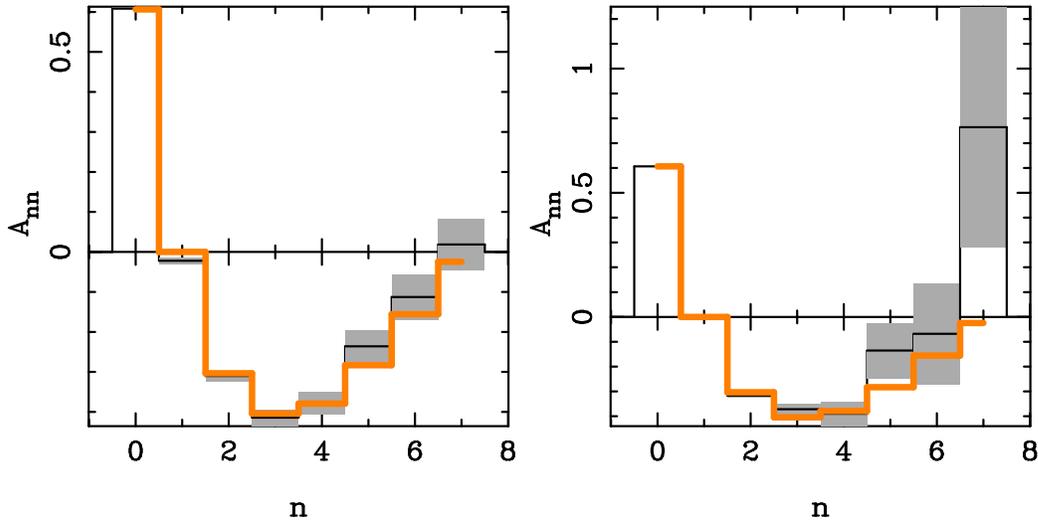
Figure 19: Homodyne tomography of the quantum operation A corresponding to the unitary displacement of one mode of the radiation field. Diagonal elements A_{nn} (shown by thin solid line on an extended abscissa range,) with their respective error bars in gray shade, compared to the theoretical probability (thick solid line). Similar results are obtained for all upper and lower diagonals of the quantum operation matrix A. The reconstruction has been achieved using an entangled state $|\psi\rangle\!\rangle$ at the input corresponding to parametric downconversion of vacuum with mean thermal photon $\bar{n}$ and quantum efficiency at homodyne detectors η. Top: $z = 1$, $\bar{n} = 5$, $\eta = 0.9$, and 150 blocks of 10^4 data have been used. Bottom: $z = 1$, $\bar{n} = 3$, $\eta = 0.7$, and 300 blocks of $2 \cdot 10^5$ data have been used. The bottom plot corresponds to the same parameters of the experiment in Ref. M. Vasilyev, S.-K. Choi, P. Kumar, and G. M. D'Ariano, Phys. Rev. Lett. **84** 2354 (2000).
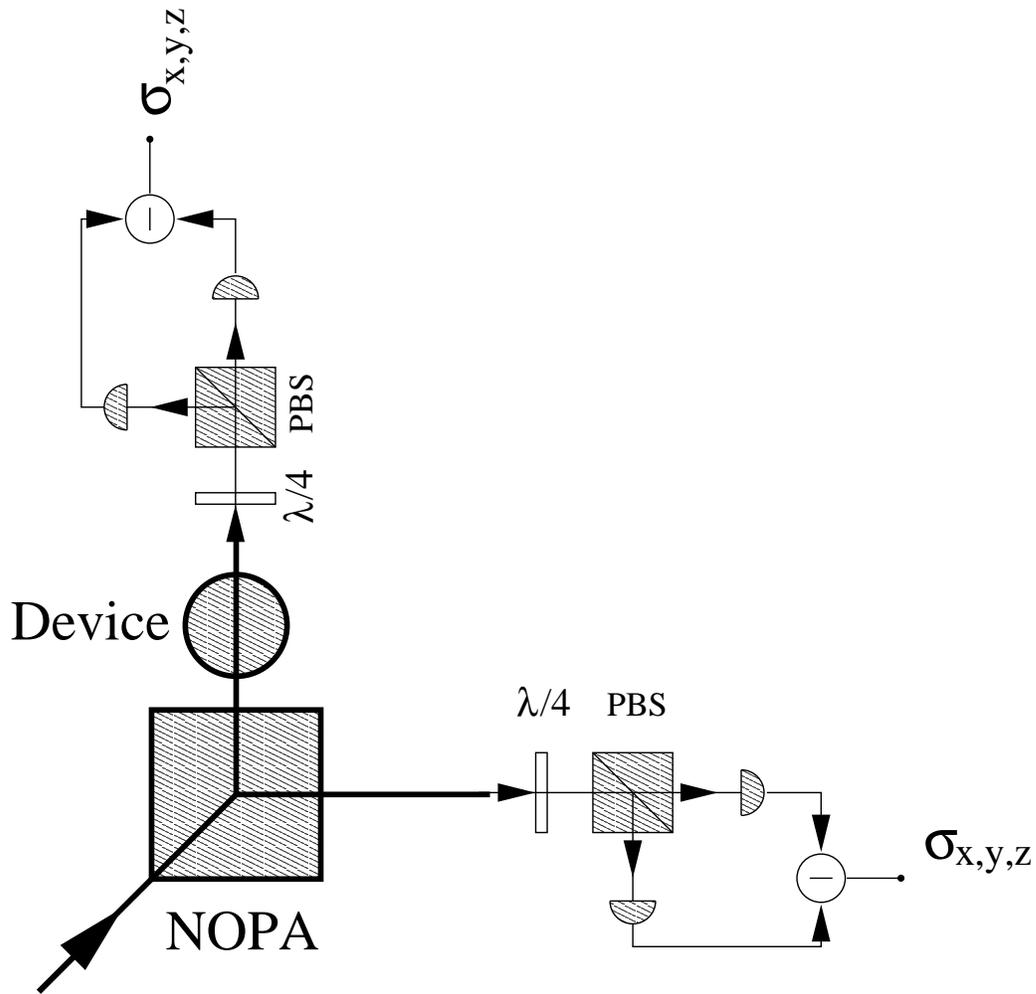
- Tomography of a single qubit quantum device

Figure 20: Experiment in progress in Roma La Sapienza, F. De Martini lab.

- The tomography of quantum operation would also be possible by **scanning over a complete set** of orthogonal input states (such as photon number states) along with linear superpositions of two of them with ± 1 relative phases. This, however, is **unfeasible** experimentally, whereas the entangled state is experimentally feasible!

- Our method exploits the *quantum parallelism* of entanglement, with **a single entangled state playing the role of a varying input state**, thus overcoming the practically insolvable problem of availability of all possible input states for the tomographic analysis of the quantum operation.

Conclusions

1. Quantum Tomography is a perfectly unbiased method for universal estimation of any ensemble average of an arbitrary quantum system, with totally unknown state. No assumptions and approximations.

2. Works with many modes/particles, either distinguishable or indistinguishable.

3. General method for deconvolving instrumental noise available;

4. Max-lik and averaging strategies available;

5. Error-improving adaptive methods available;

6. Tomography of Quantum Operations available.